Electron-Hole Asymmetric Chiral Breakdown of Reentrant Quantum Hall States

A. V. Rossokhaty,[1,2,3] Y. Baum,[4] J. A. Folk,[1,2,*] J. D. Watson,[5,6] G. C. Gardner,[6,7] and M. J. Manfra[5,6,8,7]
[1]Stewart Blusson Quantum Matter Institute, University of British Columbia, Vancouver, British Columbia V6T1Z4, Canada
[2]Department of Physics and Astronomy, University of British Columbia, Vancouver, British Columbia V6T1Z4, Canada
[3]Department of Radio Engineering and Cybernetics, Moscow Institute of Physics and Technology, Dolgoprudny, Moscow Region 141700, Russia
[4]Department of Condensed Matter Physics, Weizmann Institute of Science, Rehovot 76100, Israel
[5]Department of Physics and Astronomy, and Station Q Purdue, Purdue University, West Lafayette, Indiana 47907, USA
[6]Birck Nanotechnology Center, Purdue University, West Lafayette, Indiana 47907, USA
[7]School of Materials Engineering, Purdue University, West Lafayette, Indiana 47907, USA
[8]School of Electrical and Computer Engineering, Purdue University, West Lafayette, Indiana 47907, USA
(Received 18 December 2015; revised manuscript received 26 May 2016; published 11 October 2016)

Reentrant integer quantum Hall (RIQH) states are believed to be correlated electron solid phases, although their microscopic description remains unclear. As bias current increases, longitudinal and Hall resistivities measured for these states exhibit multiple sharp breakdown transitions, a signature unique to RIQH states. A comparison of RIQH breakdown characteristics at multiple voltage probes indicates that these signatures can be ascribed to a phase boundary between broken-down and unbroken regions, spreading chirally from source and drain contacts as a function of bias current and passing voltage probes one by one. The chiral sense of the spreading is not set by the chirality of the edge state itself, instead depending on electron- or holelike character of the RIQH state.

DOI: 10.1103/PhysRevLett.117.166805

A variety of exotic electronic states emerges in high mobility 2D electron gases (2DEGs) at very low temperature and in a large out-of-plane magnetic field. The most robust are the integer quantum Hall states, described by discrete and highly degenerate Landau levels. When the uppermost Landau level is partially filled, electrons in that level may reassemble into a fractional quantum Hall (FQH) liquid [1–3] or condense into charge-ordered states, from Wigner crystals to nematic stripe phases [4–13]. Such charge-ordered states, or electron solids, are observed primarily above filling factor $\nu = 2$, where Coulomb effects are strong in comparison to magnetic energy scales. They are believed to be collective in nature [14], prone to thermodynamic phase transitions like melting or freezing of a liquid.

Numerical simulations of electron solids indicate alternating regions of neighboring integer filling factors with dimensions on the order of the magnetic length [15,16]. When the last Landau level is less than half filled, the electron solid takes the form of "bubbles" of higher electron density in a sea of lower density (an electronlike phase). Above half filling, the bubbles are of lower electron density, giving a holelike phase. Insulating bubble phases lead to "reentrant" transitions of the Hall resistivity up or down to the nearest integer quantum Hall plateau, giving rise to the reentrant integer quantum Hall (RIQH) effect.

The microscopic description and thermodynamics of RIQH states remain topics of great interest [12,14–17]. Most experimental input into these questions has come from monitoring RIQH state collapse at elevated temperature or high current bias [14,17–21]. The temperature-induced transition out of insulating RIQH states is far more abrupt than would be expected for activation of a gapped quantum Hall liquid, consistent with their collective nature. RIQH collapse at elevated temperature is apparently a melting transition of the electronic system out of the electron solid state [14].

Elevated current biases induce transitions out of the insulating RIQH state that occur via sharp resistance steps, a phenomenon that has been interpreted in terms of sliding dynamics of depinned charge density waves [22] or alignment of electron liquid crystal domains by the induced Hall electric field [17]. These interpretations assume that bias-induced phase transitions happen homogeneously across the sample. On the other hand, finite currents through a quantum Hall sample generate highly localized Joule heating. Considering the collective nature of RIQH states, this suggests a mechanism for forming inhomogeneous phases across a macroscopic sample.

Here, we show that resistance signatures of high current breakdown for RIQH states reflect a macroscopic phase separation induced by the bias. That is, the breakdown process itself is sharply inhomogeneous, with the electronic system after breakdown spatially fractured into regions that are either melted (conducting) or frozen (insulating). For all RIQH states from $\nu = 2$ to $\nu = 8$, the breakdown propagates clockwise or counterclockwise from the source and drain contacts with a sense that depends on the electron- or holelike character of the particular RIQH state. The data are explained by a phase boundary between frozen and melted regions that spreads around the chip following the location of dissipation hot spots.

Measurements were performed on a 300 Å symmetrically doped GaAs/AlGaAs quantum well with low temperature electron density $n_s = 3.1 \times 10^{11}$ cm^{-2} and mobility 15×10^6 cm^2/V s [23]. Electrical contact to the 2DEG was achieved by diffusing indium beads into the corners and sides of the 5×5 mm chip [Fig. 1(a)]. FQH characteristics were optimized following Ref. [24]. Differential resistances $R \equiv dV/dI_b$ for various contact pairs were measured at 13 mK by lock-in amplifier with an ac current bias $I_{ac} =$ 5 nA at 71 Hz. A dc current bias I_{dc} was added to the ac current in many cases. At zero dc bias, characteristic R_{xx} and R_{xy} traces over $2 < \nu < 3$ show fragile FQH states as well as

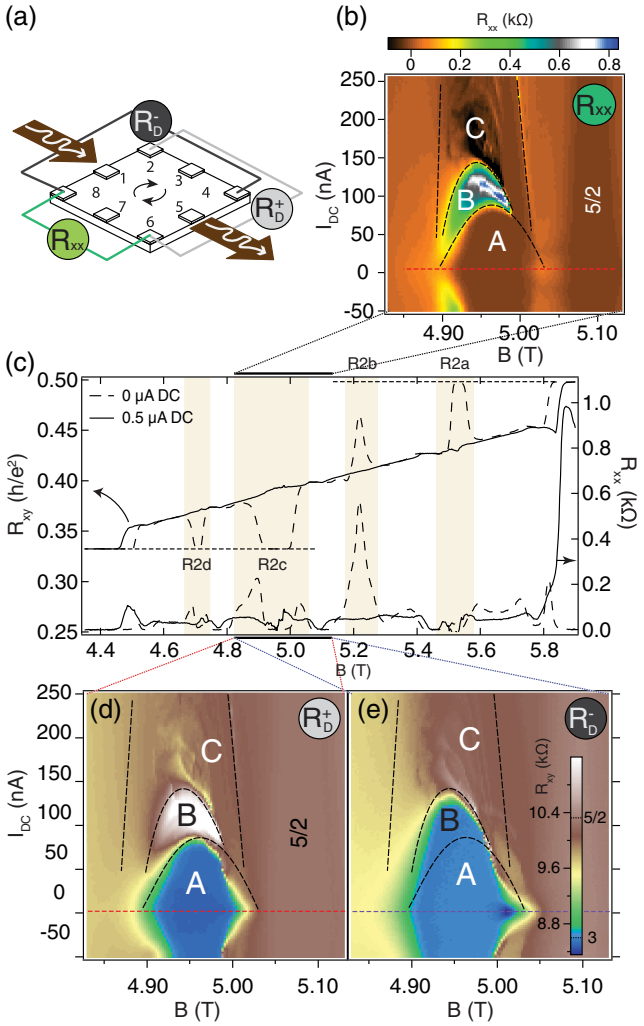

FIG. 1. (a) Measurement schematic combining ac (wiggly arrow) and dc (solid arrow) current bias through contacts 1 and 5. $R_{xx} = dV_{86}/dI$, $R_D^+ = dV_{26}/dI$, and $R_D^- = dV_{84}/dI$. Curved arrows indicate edge state chirality. (b) Evolution of R_{xx} with dc bias for the $R2c$ reentrant and $\nu = 5/2$ FQH state, showing breakdown regions A, B, and C. (c) R_{xx} and R_{xy} (dV_{37}/dI) for filling factors $\nu = 2$–3, showing the breakdown at high dc bias. (d),(e) Simultaneous measurements of (d) R_D^+ and (e) R_D^-, taken together with data in (b). Dashed lines are guides to the eye, denoting identical $\{B, I_{dc}\}$ parameters in (b), (d), and (e).

four RIQH states, labeled $R2a$–$R2d$ [Fig. 1(c)] (refer to the Supplemental Material for a complete labeling of reentrant states [25]). At high current bias, the RIQH states disappear, with R_{xy} moving close to the classical Hall resistance, while most fractional states remain well resolved.

The RIQH breakdown process can be visualized in 2D resistance maps versus I_{dc} and magnetic field. Figure 1 presents several such maps for the holelike $R2c$ state ($\nu \sim 2.58$), where the Hall resistance reenters to the integer value $R_{xy} = h/3e^2$. Breakdown transitions for R_{xx} [Fig. 1(b)] divide the map into three distinct subregions (A, B, C), similar to observations by others [17,21]. Region A is characterized by very low R_{xx}: here, the electron solid state is presumably pinned and completely insulating. The sharp transition to region B corresponds to a sudden rise in R_{xx}, while for higher bias (region C), the differential resistance drops again to a very small value.

The sharp transitions visible in the RIQH state breakdown [Fig. 1(b)] are absent from the neighboring $\nu = 5/2$ state. Considering the range of filling factors investigated here (see the Supplemental Material [25]) and data from many cooldowns, this behavior was observed consistently in RIQH states, but never in fractional states, pointing to distinct thermodynamic properties for the two ground states. Qualitative signatures at each pair of voltage probes (R_{xx}, R_{xy}, or the diagonal measurements R_D^+ or R_D^- [Fig. 1(a)]) did not depend on the specific contacts used in the measurement but only on the arrangement of the contacts with respect to source or drain current leads (see the Supplemental Material [25]).

The observation of sharp delineations in the resistance of a macroscopic sample, measured between voltage probes separated by 5 mm, might seem to imply that the entire sample must suddenly change its electronic state for certain values of bias current and field. Then, one would expect simultaneous jumps in resistance monitored at any pair of voltage probes, albeit by differing amounts. Comparing the three pairs of voltage probes in Figs. 1(b),1(d), and 1(e), one sees immediately that this is not the case. R_D^+ exhibits transitions at precisely the same parameter pairs $\{B, I_{dc}\}$ as R_{xx}, but for R_D^- no resistance change is observed at the dashed line corresponding to the R_{xx} A-B transition. It is well known that R_D^+ and R_D^- can be different when the sample is inhomogeneous [26,27]. However, the extremely high quality 2DEG samples measured here are intrinsically homogeneous, as evidenced by the visibility of closely spaced and fragile fractional states.

R_D^+ and R_D^- contacts are distinguished by the chirality of quantum Hall edge states: moving from source or drain contacts following the edge state chirality, one first comes to the R_D^+ contacts, then to R_{xy} contacts in the middle of the sample, and finally to the R_D^- contacts. The bias where the $A - B$ transition occurs for R_D^+, R_{xy}, and R_D^- simply follows the spatial distribution of the respective voltage contacts, as shown in Fig. 2(a). An analogous breakdown behavior

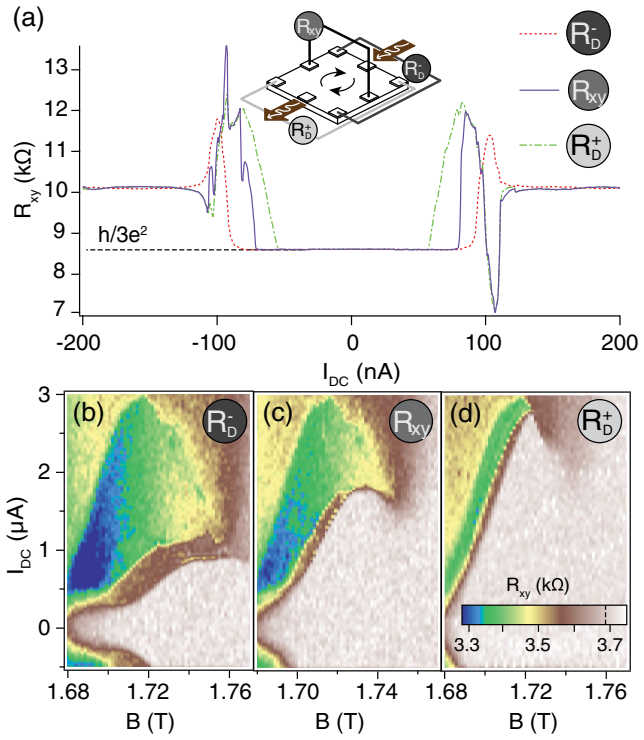

FIG. 2. (a) Simultaneous measurements showing the evolution of R_D^+, R_{xy}, and R_D^-, with dc bias, in the middle of the $R2c$ reentrant state ($I_{ac} = 5$ nA); note that this measurement uses a contact configuration rotated by 90° from Fig. 1. Evolution of (b) R_D^-, (c) R_{xy}, and (d) R_D^+ for the $R7a$ reentrant state with dc bias.

(breakdown bias for R_D^+ lower than for R_{xy}, lower than for R_D^-) was consistently observed for every holelike RIQH state. For all electronlike states, a similar breakdown progression was observed but the order was opposite: breakdown bias for R_D^+ higher than for R_{xy}, higher than for R_D^-. Figures 2(b)–2(d) show this progression for $R7a$, the electronlike RIQH state between $\nu = 7$ and $\nu = 8$ (see the Supplemental Material [25]).

The correlation between electron or hole character and breakdown chirality offers an important hint as to the origin of this effect. Edge state chirality is fixed by magnetic field direction and would not suddenly reverse when crossing half filling for each Landau level. Instead, we propose an explanation based on localized dissipation in the quantum Hall regime—so-called hot spots—any time a significant bias is applied.

Driving a current I_b through a sample in the integer quantum Hall (IQH) regime, where ρ_{xx} is close to 0 but R_{xy} is large, requires a potential difference $R_{xy}I_b$ between source and drain. This potential drops entirely at the source and drain contacts (no voltage drop can occur within the sample since $\rho_{xx} \to 0$). Specifically, the voltage drops where the current carried along a few-channel edge state is dumped into the metallic source or drain contact—a region of effectively infinite filling factor.

For a sample in the reentrant IQH regime, with $\rho_{xx} \to 0$ as before, hot spots again appear at any location where current flows from a region of higher to lower R_{xy}. But now, the local value of R_{xy} is strongly temperature dependent, with a sharp melting transition in both longitudinal and transverse resistances [14]. The electronlike $R2a$ reentrant state, for example, has $R_{xy}^{\text{reentrant}} = h/2e^2$ in the low temperature, low bias limit [Fig. 1(c)], but at higher temperature or bias, the state melts to $R_{xy}^{\text{melted}} \simeq h/2.35e^2$. In general, electronlike states have $R_{xy}^{\text{melted}} < R_{xy}^{\text{reentrant}}$, whereas holelike states have $R_{xy}^{\text{melted}} > R_{xy}^{\text{reentrant}}$.

At low current bias in the RIQH regime, the entire sample is effectively at integer ν, and only the two IQH hot spots are observed, at source and drain contacts. As the bias increases, the regions around the two IQH hot spots melt and an extra two RIQH hot spots appear where current passes into or out of the melted regions. This framework, with the 5 × 5 mm sample broken into macroscopic frozen and melted regions due to dissipation in local hot spots at the boundary, can explain why the breakdown phenomenology was observed only for RIQH states. A crucial ingredient in this picture is that current flowing from source to drain passes through a well-defined phase boundary, with a large and discrete jump in R_{xy}, even when there are continuous thermal gradients across the sample. This results from sharp electronic phase transitions, which are expected for correlated RIQH states and yield sharp jumps in R_{xx} and R_{xy} with elevated temperature, in contrast to activated behavior of FQH states.

Classical simulations of dissipation in a sample broken into regions with differing R_{xy} (in this case, $R_{xy}^{\text{reentrant}}$ and R_{xy}^{melted}) confirm the connection between hot-spot location, edge chirality, and changes in filling factor. Hot spots appear where current passes from melted into frozen regions for the holelike case in Fig. 3 because $R_{xy}^{\text{melted}} > R_{xy}^{\text{reentrant}}$; they appear on the opposite sides of the melted regions for electronlike states where $R_{xy}^{\text{melted}} < R_{xy}^{\text{reentrant}}$

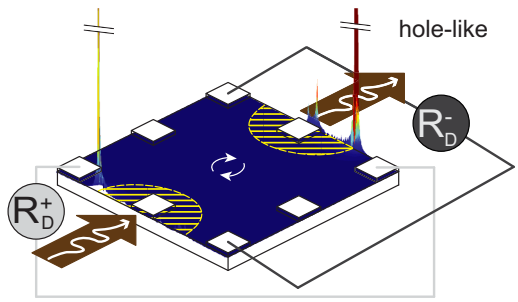

FIG. 3. Classical simulation of dissipation (color scale and 3D projection in a.u.) due to current flow in a sample with regions of different R_{xy}. Hatched semicircles are melted states near each contact with $R_{xy} = h/(2.5e^2)$; the bulk (dark blue) is the (frozen) reentrant state with $R_{xy} = h/(3e^2)$. The simulation captures hot-spot locations but does not accurately capture relative magnitudes of dissipation in different hot spots.

(see the Supplemental Material [25]). The semicircular melted regions in Fig. 3 are defined by the simulation inputs; in reality, these regions would be expected to spread in the direction of extra heating, that is, following the hot-spot locations, until heat flow into the substrate balances the hot-spot dissipation.

Consider as an example the $R2c$ measurements in Fig. 1. RIQH hot spots for holelike states are downstream from source and drain contacts following edge state chirality (Fig. 3), so the boundaries between melted and frozen regions propagate clockwise from contacts 1 and 5 around the sample edge. Within region A, we speculate that the hot spots have not yet passed a voltage probe, so no change is observed in R_{xx}, R_D^+, or R_D^-. When the hot spots pass voltage probes 2 and 6, used for R_{xx} and R_D^+, both resistances register a jump due to the potential drop at the hot spot. R_D^- is unaffected because the potential drop did not pass into or out of the contact pair (4, 8). This mechanism also explains the progression of the transition between A and B regions for $\{R_D^+, R_{xy}, R_D^-\}$ in Fig. 2. For $R2c$ [Fig. 2(a)], the hot spot first passes the R_D^+ probe, then the R_{xy} contact, then the R_D^- contact; for the electronlike $R7a$ [Figs. 2(b)–2(d)], the hot spot propagates against the edge state chirality, so it passes the R_D^- probe, then R_{xy}, then R_D^+.

Finally, we turn to a measurement configuration that has been used to investigate possible anisotropy in the electron solid at high bias, when the Hall electric field is large. Reference [17] compared R_{xx} measured parallel or perpendicular to a large dc current bias, by rotating the R_{xx} voltage probes and ac current bias contacts by 90° with respect to the dc bias contacts [Figs. 4(a) and 4(b)]. It was observed that the low R_{xx} region A extended to much higher bias for the (ac⊥dc) orientation, compared to the conventional (ac‖dc) orientation. While Ref. [17] focused on $R4$ states exclusively, we found analogous behavior for all reentrant states measured [see, e.g., Figs. 4(c) and 4(d)].

This behavior can be simply explained by the hot-spot-movement mechanism outlined above, without resorting to induced anisotropy in the electron solid. Figure 4(a) and 4(b) schematics include dashed lines to show hypothetical melted-frozen boundaries for an electronlike state at intermediate bias, with associated RIQH hot spots (⋆). The melted region surrounds the dc (not ac) current contacts because the measurement is done in the limit of vanishing ac bias. The boundary is not symmetric around the dc contacts as the melted region is presumed to have propagated counterclockwise (for electronlike states) from the contacts, following the ⋆ hot-spot locations.

The local ac potential along the edge of the sample drops sharply when passing the ac source and drain (the conventional IQH hot spots), but a second smaller potential drop occurs at each ⋆ when the melted region includes an ac source or drain [e.g., Fig. 4(a)]. For this distribution of melted and frozen phases, there is a potential drop between

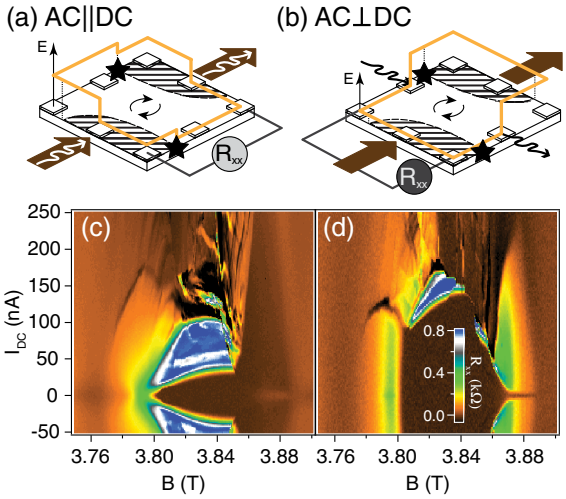

FIG. 4. Comparison of measurement geometries (a) ac‖dc and (b) ac⊥dc; arrows label source and drain contacts for dc (solid arrows) and ac (wiggly arrows) bias, and edge state chirality (curved arrows). The vertical axis E denotes local ac edge state potential (yellow line). Hatched areas are hypothetical melted regions for an electronlike reentrant state at intermediate dc bias $I_{dc} \sim 50$ nA in (c) and (d). Hot spots at the melted-frozen boundary indicated by ⋆. (c),(d) $R3a$ R_{xx} maps in the (I_{dc}, B) plane for (c) ac‖dc and (d) ac⊥dc measurement.

the R_{xx} voltage probes in Fig. 4(a) but not in Fig. 4(b), so large R_{xx} would be registered only when ac‖dc. A configuration like that shown in Figs. 4(a) and 4(b) might correspond to intermediate bias, around 50 nA in Figs. 4(c) and 4(d), thus explaining the large region of high R_{xx} in Fig. 4(c) that appears only above 100 nA in Fig. 4(d).

In conclusion, we demonstrated that bias-induced breakdown of the RIQH effect is inhomogeneous across mm-scale samples and propagates chirally from source and drain contacts with a sense that depends on the electron- or holelike character of the reentrant state. This phenomenon appears to result from a thermal runaway effect due to phase segregation and dissipation hot spots; it was observed only in (correlated) RIQH states, not fractional or integer states, pointing to their qualitatively distinct thermodynamic properties. This experiment shows the danger in interpreting macroscopic measurements at a microscopic level, especially where electronic phase transitions are sharp. On the other hand, it demonstrates the power of using breakdown characteristics as a probe into thermal properties of correlated electron states. Looking ahead, it would be particularly interesting to investigate combined Corbino and Hall bar geometries, where hot-spot-induced breakdown could be included or avoided as desired. Adding multiple small contacts within the interior of a sample would enable melted and frozen phases to be measured separately and the nature of the transition region to be probed directly.

The authors acknowledge helpful discussions with J. Smet and A. Stern. Experiments at UBC were supported by Natural Sciences and Engineering Research Council of Canada (NSERC), Canada Foundation for Innovation (CFI), and Canadian Institute for Advanced Research (CIFAR). The molecular beam epitaxy growth at Purdue is supported by the U.S. Department of Energy, Office of Basic Energy Sciences, Division of Materials Sciences and Engineering, under Grant No. DE-SC0006671.

*jfolk@physics.ubc.ca

[1] R. B. Laughlin, Phys. Rev. Lett. **50**, 1395 (1983).
[2] B. I. Halperin, P. A. Lee, and N. Read, Phys. Rev. B **47**, 7312 (1993).
[3] D. C. Tsui, H. L. Stormer, and A. C. Gossard, Phys. Rev. Lett. **48**, 1559 (1982).
[4] R. Du, D. Tsui, H. Stormer, L. Pfeiffer, K. Baldwin, and K. West, Solid State Commun. **109**, 389 (1999).
[5] M. P. Lilly, K. B. Cooper, J. P. Eisenstein, L. N. Pfeiffer, and K. W. West, Phys. Rev. Lett. **82**, 394 (1999).
[6] W. Pan, J. S. Xia, E. D. Adams, R. R. Du, H. L. Stormer, D. C. Tsui, L. N. Pfeiffer, K. W. Baldwin, and K. W. West, Physica (Amsterdam) **298B**, 113 (2001).
[7] A. A. Koulakov, M. M. Fogler, and B. I. Shklovskii, Phys. Rev. Lett. **76**, 499 (1996).
[8] M. M. Fogler, A. A. Koulakov, and B. I. Shklovskii, Phys. Rev. B **54**, 1853 (1996).
[9] J. P. Eisenstein, K. B. Cooper, L. N. Pfeiffer, and K. W. West, Phys. Rev. Lett. **88**, 076801 (2002).
[10] J. S. Xia, W. Pan, C. L. Vicente, E. D. Adams, N. S. Sullivan, H. L. Stormer, D. C. Tsui, L. N. Pfeiffer, K. W. Baldwin, and K. W. West, Phys. Rev. Lett. **93**, 176809 (2004).
[11] G. A. Csáthy, J. S. Xia, C. L. Vicente, E. D. Adams, N. S. Sullivan, H. L. Stormer, D. C. Tsui, L. N. Pfeiffer, and K. W. West, Phys. Rev. Lett. **94**, 146801 (2005).
[12] M. O. Goerbig, P. Lederer, and C. M. Smith, Phys. Rev. B **69**, 115327 (2004).
[13] N. Shibata and D. Yoshioka, J. Phys. Soc. Jpn. **72**, 664 (2003).
[14] N. Deng, A. Kumar, M. J. Manfra, L. N. Pfeiffer, K. W. West, and G. A. Csáthy, Phys. Rev. Lett. **108**, 086803 (2012).
[15] E. Fradkin and S. A. Kivelson, Phys. Rev. B **59**, 8065 (1999).
[16] B. Spivak and S. A. Kivelson, Ann. Phys. (Amsterdam) **321**, 2071 (2006).
[17] J. Göres, G. Gamez, J. H. Smet, L. Pfeiffer, K. West, A. Yacoby, V. Umansky, and K. von Klitzing, Phys. Rev. Lett. **99**, 246402 (2007).
[18] W. E. Chickering, J. P. Eisenstein, L. N. Pfeiffer, and K. W. West, Phys. Rev. B **87**, 075302 (2013).
[19] K. B. Cooper, M. P. Lilly, J. P. Eisenstein, L. N. Pfeiffer, and K. W. West, Phys. Rev. B **60**, R11285 (1999).
[20] K. B. Cooper, J. P. Eisenstein, L. N. Pfeiffer, and K. W. West, Phys. Rev. Lett. **90**, 226803 (2003).
[21] S. Baer, C. Rössler, S. Hennel, H. C. Overweg, T. Ihn, K. Ensslin, C. Reichl, and W. Wegscheider, Phys. Rev. B **91**, 195414 (2015).
[22] C. Reichhardt, C. J. O. Reichhardt, and A. R. Bishop, Europhys. Lett. **72**, 444 (2005).
[23] M. J. Manfra, Annu. Rev. Condens. Matter Phys. **5**, 347 (2014).
[24] M. Samani, A. V. Rossokhaty, E. Sajadi, S. Lüscher, J. A. Folk, J. D. Watson, G. C. Gardner, and M. J. Manfra, Phys. Rev. B **90**, 121405 (2014).
[25] See Supplemental Material at http://link.aps.org/supplemental/10.1103/PhysRevLett.117.166805 for further data, extending what is shown in the main text figures to other reentrant states and other sample measurement configurations. Simulation details are also included.
[26] C. W. J. Beenakker and H. van Houten, Solid State Phys. **44**, 1 (1991).
[27] M. Büttiker, Phys. Rev. B **38**, 9375 (1988).